

MSNav: Zero-Shot Vision-and-Language Navigation with Dynamic Memory and LLM Spatial Reasoning

Chenghao Liu^{1*}, Zhimu Zhou^{1*}, Jiachen Zhang¹, Minghao Zhang², Songfang Huang^{1†}, Huiling Duan¹

¹School of Advanced Manufacturing and Robotics, Peking University, ²Institute for Network Sciences and Cyberspace, Tsinghua University

Abstract

Vision-and-Language Navigation (VLN) requires an agent to interpret natural language instructions and navigate complex environments. Current approaches often adopt a "black-box" paradigm, where a single Large Language Model (LLM) makes end-to-end decisions. However, it is plagued by critical vulnerabilities, including poor spatial reasoning, weak cross-modal grounding, and memory overload in long-horizon tasks. To systematically address these issues, we propose Memory Spatial Navigation(MSNav), a framework that fuses three modules into a synergistic architecture, which transforms fragile inference into a robust, integrated intelligence. MSNav integrates three modules: Memory Module, a dynamic map memory module that tackles memory overload through selective node pruning, enhancing long-range exploration; Spatial Module, a module for spatial reasoning and object relationship inference that improves endpoint recognition; and Decision Module, a module using LLM-based path planning to execute robust actions. Powering Spatial Module, we also introduce an Instruction-Object-Space (I-O-S) dataset and fine-tune the Qwen3-4B model into Qwen-Spatial (Qwen-Sp), which outperforms leading commercial LLMs in object list extraction, achieving higher F1 and NDCG scores on the I-O-S test set. Extensive experiments on the Room-to-Room (R2R) and REVERIE datasets demonstrate MSNav's state-of-the-art performance with significant improvements in Success Rate (SR) and Success weighted by Path Length (SPL).

1 Introduction

We hope that VLN agents can eventually achieve navigating complex environments with remarkable efficiency. For example, when instructed to "reach the kitchen's refrigerator," an ideal VLN agent can visualize the kitchen layout, focus on key landmarks, and filter out irrelevant details from memory. However, existing LLM-based Zero-Shot VLN (ZS-VLN) solutions frequently falter in complex, long-distance tasks and scenarios with ambiguous endpoints (Zhou, Hong, and Wu 2023; Long et al. 2023; Chen et al. 2024).

Inspired by the failures in prior VLN solutions, we propose Memory Spatial Navigation(MSNav), a framework together with dynamic memory, LLM spatial reasoning and

*These authors contributed equally to this work, ordered by randomly dice rolling.

†Corresponding author: hsf@pku.edu.cn

LLM-based planning, which transforms fragile black-box inference into a robust, integrated intelligence. MSNav integrates three modules:(1) Memory Module, creating a dynamic topological map that selectively retains important spatial information while discarding outdated or irrelevant details; (2) Spatial Module, presenting reasonable spatial imagination and reasoning capabilities, analyzing instructions and infers spatial layouts from linguistic cues, and enhancing the agent's ability to understand environmental context; and (3) Decision Module, advanced LLMs to determine navigation actions based on instructions, processed observations, object spatial layouts, and map information.

Additionally, we construct an Instruction-Object-Space (I-O-S) dataset, derived from oracle paths across indoor environments, to support instruction analysis and spatial reasoning. We have also fine-tuned the Qwen3-4B model(Yang et al. 2025) on this I-O-S dataset to create the Qwen-Sp model, which can analyze language instructions for VLN tasks, extract and reason about objects along the navigation path, and infer spatial layouts of objects at the destination. Extensive experiments on the Room-to-Room (R2R) and REVERIE datasets (Anderson et al. 2018; Qi et al. 2020) demonstrate MSNav's state-of-the-art performance, with significant gains in Success Rate (SR) and Success weighted by Path Length (SPL).

Our contributions are:

- We introduce MSNav, achieving state-of-the-art performance with a 5.1% improvement in SR and 5.0% in SPL on the R2R subset (Anderson et al. 2018).
- We present the I-O-S dataset, comprising 28,414 samples, enabling fine-grained analysis of navigation instructions.
- We develop Qwen-Sp, outperforming leading commercial LLMs (OpenAI 2024; Google DeepMind 2025; xAI 2025) in the task of object extraction, achieving a higher F1 score (0.316 vs. 0.270 for GPT-4o) and NDCG score (0.388 vs. 0.325 for GPT-4o) on the I-O-S test set.
- We demonstrate the versatility of the Spatial Module, which can be seamlessly integrated into other VLN frameworks to enhance their performance, whether map-based or not.

2 Related Work

Vision-and-Language Navigation Vision-and-Language Navigation (VLN) tasks an agent with following natural language instructions in 3D environments (Anderson et al. 2018; Krantz et al. 2020; Chen et al. 2019; Qi et al. 2020). Foundational research in VLN was dominated by supervised methods focusing on cross-modal alignment (Hao et al. 2020; Hong et al. 2021a; Chen et al. 2021b, 2020; Li et al. 2020) and was supplemented by techniques like data augmentation, specialized training, and self-correction (Fried et al. 2018; Tan, Yu, and Bansal 2019; Wang et al. 2023, 2019; Huang et al. 2019; Ke et al. 2019; Ma et al. 2019). A central component has always been spatial memory, implemented via metric maps (Thrun 1998; Fuentes-Pacheco, Ruiz-Ascencio, and Rendon-Mancha 2015) or efficient topological graphs to manage historical information and environmental structure (Chen et al. 2021c; Deng, Narasimhan, and Russakovsky 2020; Chen et al. 2021a, 2022b).

Large Language Models in VLN Large Language Models (LLMs) (Brown et al. 2020; OpenAI 2023) have introduced a new paradigm, enabling Zero-Shot VLN (ZS-VLN) where they serve as out-of-the-box planners. Seminal works like NavGPT (Zhou, Hong, and Wu 2023) demonstrated this feasibility, while subsequent approaches like Discuss-Nav (Long et al. 2023) and MapGPT (Chen et al. 2024) enhanced LLM reasoning by incorporating multi-agent dialogue or topological maps. In parallel, LLMs are also being successfully fine-tuned for navigation (Pan et al. 2023; Lin et al. 2024). Effective prompting remains crucial across all LLM-based methods to elicit strong performance (Wei et al. 2022; Kojima et al. 2022; Yao et al. 2022).

3 Methodology

Task Description VLN tasks require an agent to interpret a natural language instruction $I = \{w_1, w_2, \dots, w_L\}$ and navigate a 3D environment to a target location. At each step t , given the current pose p_t , the simulator provides several neighboring viewpoints that are currently navigable. The agent observes its state s_t , including a set of navigable viewpoints $\mathcal{V}_t = \{v_{t,i}\}_{i=1}^K$, where K is the number of navigable viewpoints, and visual observations O , and selects an action a_t from a discrete action space A_t (e.g., navigate to an adjacent viewpoint or stop). The action is sent to the control module to execute the corresponding movement. The challenge lies in grounding linguistic instructions in visual scenes to generate an action sequence $A = \{a_1, a_2, \dots, a_T\}$.

MSNav adopts a modular framework that integrates three key processes: memory, spatial reasoning, and decision-making. The framework comprises Memory Module, Spatial Module, and Decision Module, which work together to process visual and linguistic inputs efficiently, as illustrated in Figure 1. These modules have a mutual collaboration and cooperation to achieve robust and effective navigation in complex indoor environments.

3.1 Memory Module

Constructing navigation maps (Epstein et al. 2017) and a strong memory system (Baddeley and Hitch 1974; Malleret et al. 2024) is proved helpful in completing a navigation task in a complex environment. We investigated current VLN performances, noting that existing methods usually fail in prolonged tasks (Zhou, Hong, and Wu 2023; Long et al. 2023; Chen et al. 2024), particularly beyond 13 steps in the R2R dataset (Anderson et al. 2018). Excessive node accumulation in topological maps overwhelms LLM context limits, reducing success rates. Unlike prior approaches that retain all observations in an expanding map (Chen et al. 2022b; Chen et al. 2024), our Memory Module dynamically filters irrelevant nodes, sustaining performance and mitigating LLM context constraints. The overall workflow of Memory Module is illustrated in Figure 2.

Map Construction In VLN, the agent builds a real-time map of an unfamiliar environment using observations from exploration. Following prior work (Chen et al. 2022b; Chen et al. 2024), we use a topological graph $G_t = (V_t, E_t)$, where $V_t = \{v_{t,i}\}_{i=1}^K$ represents viewpoint nodes observed up to time step t , and E_t denotes navigable connections between them.

At each step t , the agent records new viewpoints and their connections based on the simulator’s feedback about neighboring nodes. These are added to an intermediate graph G_t^{tmp} , updated from the previous graph G_{t-1} . After obtaining the intermediate graph G_t^{tmp} , it is dynamically pruned to produce the final graph G_t .

Dynamic Map Pruning To maintain a compact and task-relevant topological map, Memory Module dynamically evaluates and prunes nodes from the intermediate graph G_t^{tmp} that are no longer pertinent to the navigation task. This process begins after an initial exploration phase ($t \geq t_{\text{start}}$), ensuring the map remains efficient by removing outdated or irrelevant information. By selectively filtering nodes, the Memory Module reduces memory overhead and mitigates interference from obsolete data, producing the final graph G_t .

The set $T_t \subseteq V_t^{\text{tmp}}$ represents all viewpoint nodes that the agent has visited up to time step t . This set tracks the agent’s exploration history and is used to assess node relevance.

The Memory Module identifies a subset of nodes $\mathcal{V}_{\text{assess}} \subseteq V_t^{\text{tmp}}$ for relevance evaluation based on three criteria: nodes must be *non-current*, meaning they are not the agent’s current viewpoint ($v_{t,i} \neq v_t$); they must be *previously visited*, having been explored ($v_{t,i} \in T_t$); and they must be *temporally stale*, not revisited recently, satisfying $t - \tau(v_{t,i}) > \theta_{\text{recent-visit}}$ and $t - \tau(v_{t,i}) > \theta_{\text{age}}$, where $\tau(v_{t,i})$ is the time step when node $v_{t,i}$ was last visited, $\theta_{\text{recent-visit}}$ is the minimum time elapsed since the last visit to consider a node for pruning, and θ_{age} is the threshold for determining node staleness based on its age.

Nodes in $\mathcal{V}_{\text{assess}}$ are assigned a pruning priority score $P(v_{t,i})$, which quantifies their relevance to the ongoing task:

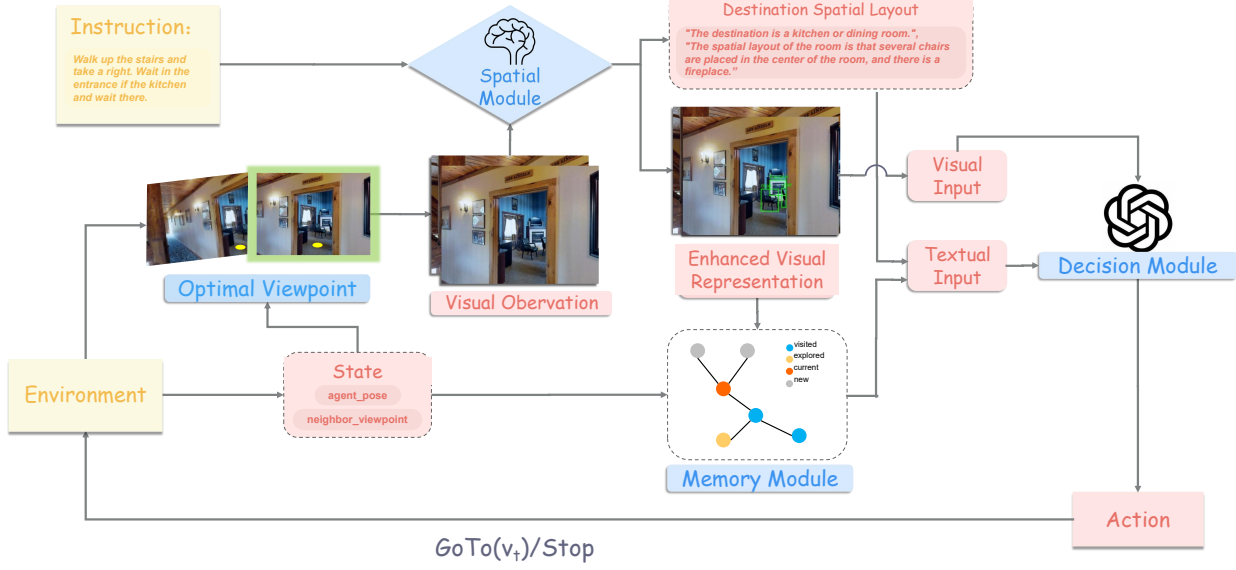


Figure 1: The MSNav architecture. The agent perceives the environment and then identifies optimal navigable viewpoint(yellow dot shows the best viewpoint that contains complete spatial information, explanation only). Memory Module maintains a topological map for long-term context. Spatial Module reasons about the target location by processing instructions and visual cues. Based on the map, layout, and current view, the Decision Module outputs navigation action(stop or proceed to a selected viewpoint), and the 'observe-reason-act' cycle repeats until task completion.

$$P(v_{t,i}) = \lambda_t f_t(v_{t,i}) + \lambda_d f_d(v_{t,i}) + \lambda_f f_f(v_{t,i}) + \lambda_{\text{dist}} f_{\text{dist}}(v_{t,i}) \quad (1)$$

where:

- $f_t(v_{t,i}) = \max(1, t - \tau(v_{t,i}) - \theta_{\text{age}})$: Measures temporal staleness, prioritizing older nodes.
- $f_d(v_{t,i}) = -\deg_{G_t^{\text{tmp}}}(v_{t,i})$: prioritizes nodes with high connectivity, as they are more critical to navigation.
- $f_f(v_{t,i}) = -|\{v_{t,j} \mid (v_{t,i}, v_{t,j}) \in E_t^{\text{tmp}} \wedge v_{t,j} \notin T_t\}|$: prioritizes nodes with fewer unexplored neighbors, indicating lower exploration potential.
- $f_{\text{dist}}(v_{t,i}) = d_{G_t^{\text{tmp}}}(v_t, v_{t,i})$: Considers the graph distance from the current viewpoint, prioritizing distant nodes.

The coefficients $\lambda_t, \lambda_d, \lambda_f, \lambda_{\text{dist}}$ balance the contributions of each factor. A higher pruning priority value indicates a greater possibility of pruning.

Based on the pruning priority scores, the top N_{remove} nodes with the highest $P(v_{t,i})$ are removed from G_t^{tmp} , yielding the final map $G_t = (V_t, E_t)$. This selective pruning ensures that the topological map remains concise, relevant, and computationally efficient, supporting robust navigation over extended periods.

Map Representation The Memory Module structures the filtered topological map $G_t = (V_t, E_t)$ into prompts for Decision Module, adapting insights from prior work (Chen et al. 2024). The prompts include: (1) Trajectory, listing

visited node identifiers in V_t ; (2) Map, detailing node connectivity in E_t ; and (3) Supplementary Information, linking nodes v_t to enhanced visual observations $O_{k^*}^e$ from Spatial Module. This ensures a concise, task-relevant spatial representation for the LLM. Detailed prompts are in Appendix.

3.2 Spatial Module

In navigation tasks, landmarks and spatial configurations at destinations contain key information to achieve precise location identification. In VLN, agents often misidentify targets, such as stopping in a hallway instead of a kitchen in R2R tasks (Anderson et al. 2018) due to weak spatial reasoning. Spatial Module addresses this by extracting task-relevant objects from instructions and inferring destination layouts. Using our I-O-S dataset, we fine-tuned Qwen3-4B into Qwen-Sp to generate accurate object lists and layouts, boosting navigation precision. The Spatial Module is shown in Figure 3. Beyond VLN, the I-O-S dataset also enhances LLMs' spatial imagination and reasoning capabilities.

I-O-S Dataset The Instruction-Object-Space (I-O-S) dataset is a novel resource designed to enhance spatial reasoning in VLN by providing structured data that links natural language instructions to objects and their spatial arrangements. Comprising 28,414 samples derived from expert trajectories in indoor environments(25,694 training samples and 2,720 test samples), the I-O-S dataset captures three key components: (1) Instructions, which are natural language navigation directives; (2) Objects, a list of task-relevant objects encountered along the trajectory or at the

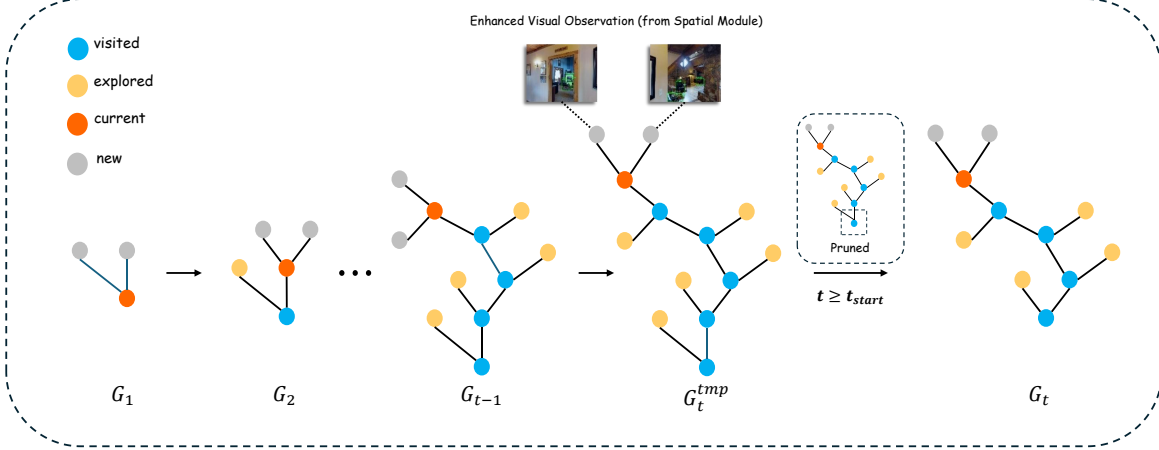


Figure 2: Memory Module, illustrating the dynamic construction and pruning of a task-relevant topological map. At step t , the Memory Module observes navigable viewpoints and uses their enhanced visual observations as representations, adding them as new nodes (gray) to the previous map G_{t-1} to form an intermediate map G_t^{tmp} ; if $t \geq t_{\text{start}}$, a pruning operation is triggered, removing N_{remove} nodes based on their pruning priority scores ($N_{\text{remove}} = 1$ in this figure), resulting in a compact map G_t .

destination; and (3) Destination Spatial Layouts, describing the relative positions of objects at the destination (e.g., “The spatial layout of the room is that several chairs are placed in the center of the room, and there is a fireplace”). Each sample in the I-O-S dataset is formatted as a tuple (I, O, S) , where I is the instruction, O is the set of objects, and S is the description of destination spatial layout.

To construct the dataset, we extracted oracle paths from indoor environments, which provide optimal navigation trajectories. Objects along the path and at the destination were identified using the simulator’s ground-truth object annotations (including object lists and their bounding box coordinates). Spatial arrangements were generated through a two-step process: first, an LLM proposed candidate layouts based on object lists and their bounding box coordinates observed in the destination scenes; second, human annotators verified and refined these layouts to ensure accuracy and consistency through iterative subset sampling. By providing fine-grained annotations, the I-O-S dataset enables models to learn extracting task-relevant objects from instructions and inferring their spatial configurations. See Appendix for details.

Spatial Reasoning Model To enable robust spatial reasoning, we developed Qwen-Sp by fine-tuning Qwen3-4B (Yang et al. 2025) on the I-O-S dataset using Low-Rank Adaptation (LoRA) (Hu et al. 2022). Qwen-Sp employs two LoRA adapters: one to extract task-relevant objects from navigation instructions (e.g., identifying “refrigerator” from “go to the kitchen’s refrigerator”) and another to infer their spatial arrangements at the destination (e.g., “the refrigerator is against the kitchen’s back wall”). Fine-tuned on 25,694 I-O-S samples, Qwen-Sp achieves superior performance in object list extraction compared to leading commercial LLMs, including GPT-4o, Gemini-2.5-Flash, and Grok3 (xAI 2025), as detailed in Section Experiments. This high-

lights Qwen-Sp’s ability to accurately identify and prioritize task-relevant objects, which is critical for effective navigation. For zero-shot REVERIE experiments (Qi et al. 2020), we avoid direct use of the fine-tuned model, instead leveraging its learned patterns to design prompts for commercial LLMs (e.g., GPT-4o). Qwen-Sp with training details is provided in the Appendix.

Visual Input Enhancement The Visual Input Enhancement component enables landmark-based pathfinding by enhancing visual observations with task-relevant objects from the spatial reasoning model’s object list, highlighting landmarks for navigation (Skaramagkas et al. 2023).

We first compute the target direction $(\theta_{\text{tg}}, \phi_{\text{tg}})$ from the agent’s current pose p_t , and selects the information-rich view visual observation O_{k^*} by finding the camera view direction (θ_k, ϕ_k) that minimizes the L_1 angular distance to this target:

$$k^* = \arg \min_{k \in \text{available views}} \mathcal{D}((\theta_k, \phi_k), (\theta_{\text{tg}}, \phi_{\text{tg}})). \quad (2)$$

Then, the component uses YOLO-World (Cheng et al. 2024), a lightweight, fast, and high-performance open-vocabulary object detection system, to annotate objects in the visual observation O_{k^*} selected, guiding the agent along the instruction-specified path. The enhanced viewpoint observation ensures that the representation encapsulates sufficient spatial information and visual features for effective navigation.

3.3 Decision Module

To harness reasoning and decision-making capabilities, we introduce the Decision Module, a module that employs an advanced LLM, GPT-4o, to facilitate high-level decision-making. At each time step t , Decision Module processes

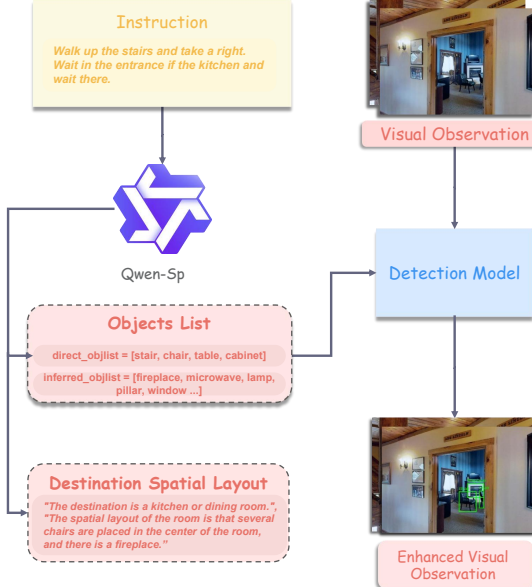


Figure 3: Spatial Module architecture depicts the pipeline for spatial reasoning. Qwen-Sp processes instructions to extract object lists and infer destination spatial layouts, while YOLO-World as detection model, enhances visual observations to highlight task-relevant objects for the agent.

the following inputs: the natural language instruction (I), specifying the navigation goal; the Memory Module context (C_t^{Memory}), including the trajectory and the map; the destination spatial layout (SL^{Spatial}) provided by Spatial Module; and other prompt information (e.g., history, previous planning, and action options, denoted as P_t). The LLM integrates these inputs to output an action a_t , which is either the selection of a neighboring viewpoint or a decision to stop:

$$a_t = \text{Decision}(I, C_t^{\text{Memory}}, SL^{\text{Spatial}}, P_t). \quad (3)$$

Our prompt design draws on insights from prior work (Chen et al. 2024) while incorporating adaptations tailored to MSNav’s framework. Full prompt structure is detailed in the Appendix. The task workflow for MSNav is shown in the Figure 4.

4 Experiments

4.1 Experimental Settings

MSNav is evaluated on the R2R (Anderson et al. 2018) and REVERIE (Qi et al. 2020) datasets, which are widely used benchmarks in zero-shot VLN setting, with the I-O-S dataset used to assess Qwen-Sp’s spatial inferring ability. MSNav is compared to NavGPT (Zhou, Hong, and Wu 2023), DiscussNav (Long et al. 2023), and MapGPT (Chen et al. 2024), using GPT-4o for a fair comparison. Qwen-Sp is also tested against GPT-4o, Gemini-2.5-Flash, and Grok3 on the I-O-S dataset. We conduct VLN experiments on the Matterport3D simulator(Chang et al. 2017). The implementation details are in the Appendix.

Evaluation Metrics Performance is assessed using the following metrics. For VLN tasks: (1) *Success Rate (SR)*, the percentage of successful episodes; (2) *Success weighted by Path Length (SPL)*, which balances success and path efficiency; (3) *Oracle Success Rate (OSR)*, the SR with an oracle stop policy; and (4) *Navigation Error (NE)*, the average distance in meters to the target. For evaluating the spatial inference capabilities of LLMs: (5) *F1 Score*, measuring precision and recall for object list extraction; and (6) *Normalized Discounted Cumulative Gain (NDCG)*, assessing the ranking quality of extracted objects. Details for the standard metrics (1-6) are in the Appendix.

Additionally, we introduce a novel metric, *Map Efficiency (ME)*, which evaluates the quality of topological maps in VLN tasks. It is defined as:

$$ME = \frac{|T_t \cap T_{\text{expert}}|}{|T_{\text{expert}}|} \cdot \frac{1}{1 + \alpha \cdot \frac{|V_t|}{|T_{\text{expert}}|}}, \quad (4)$$

where ME balances the coverage of expert path nodes (T_{expert}) by the agent’s trajectory (T_t) against the total map size (V_t), rewarding compact yet accurate maps. Step by step, we deeply analyze the performance of Memory Module’s node discard selection during task execution, and ultimately selected the penalty factor $\alpha = 0.25$.

4.2 Experimental Results

ZS-VLN Benchmark Comparison Following prior work (Zhou, Hong, and Wu 2023; Chen et al. 2024), we evaluate MSNav on the standard R2R subset consisting of 72 scenes and 216 samples (we name it as R2R-ZS uniformly), as shown in Table 1. MSNav achieves an SR of 50.9% and SPL of an 42.6%, outperforming MapGPT by 5.1% and 5.0%, respectively. Memory Module’s pruning maintains compact maps, with an ME of 40.4%, enabling stable exploration in long trajectories. Notably, MSNav’s higher OSR (7.3% higher than MapGPT) likely stems from Memory Module’s pruning, facilitating late-stage exploration without increased resource demands.

Methods	SR↑SPL↑OSR↑NE↓ME↑
NavGPT (Zhou, Hong, and Wu 2023)	36.1 31.6 40.3 6.26 -
DiscussNav (Long et al. 2023)	37.5 33.3 51.0 6.30 -
MapGPT (Chen et al. 2024)	45.8 37.6 56.5 5.31 38.0
MSNav (Ours)	50.9 42.6 63.9 5.02 40.4

Table 1: Comparison of ZS-VLN performance on the R2R-ZS. NavGPT and MapGPT results are reproduced using GPT-4o to ensure a fair comparison.

R2R Large-Scale Evaluation To compare with prior VLN and ZS-VLN work, we evaluate MSNav on the R2R full validation unseen set (11 scenes, 783 samples), as shown in Table 2. MSNav achieves an SR of 46% and an SPL of 40%, surpassing MapGPT by 2% and 5%, respectively. The relatively moderate improvements observed here can be attributed to the limited scene diversity within the 11-scene subset, which restricts the effectiveness of Memory Module’s pruning and Spatial Module’s spatial reasoning capabilities. However, MSNav’s SR outperforms three trained

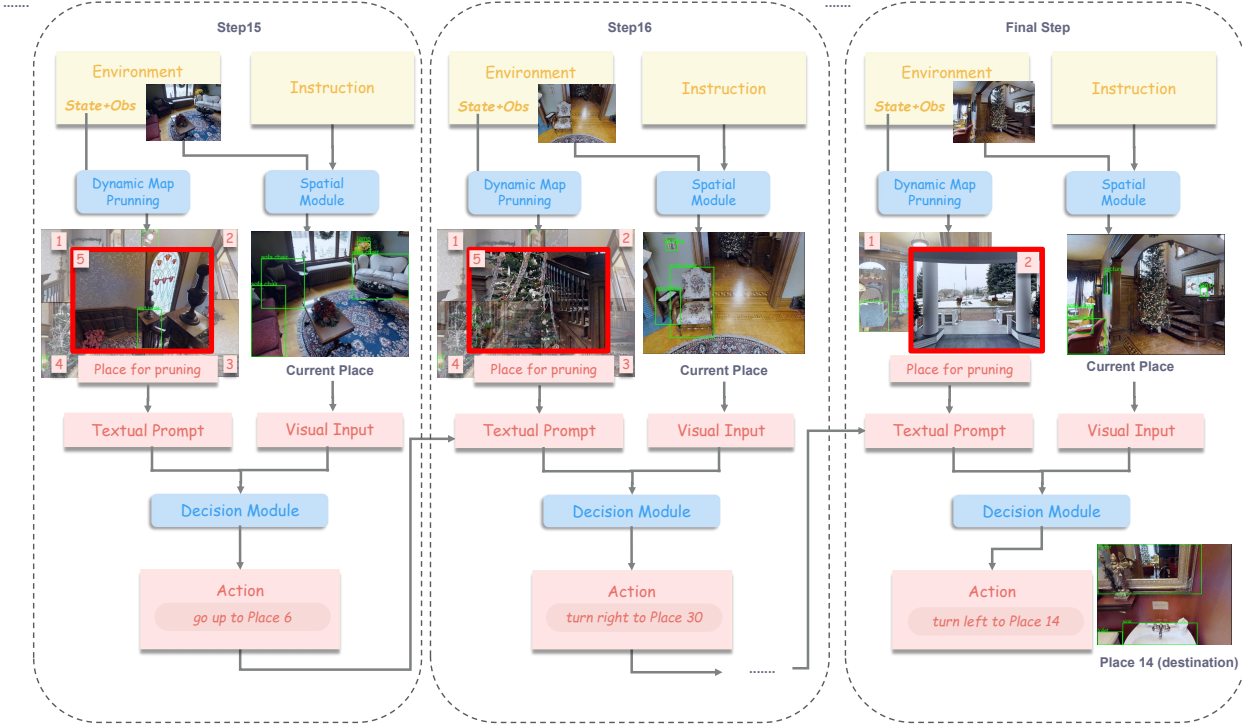


Figure 4: MSNav’s iterative VLN process (key steps shown). The Memory Module dynamically prunes environment states, forming a map for context. The Spatial Module (via Qwen-Sp) processes instructions and visual observations, inferring object lists for visual enhancement and destination spatial layouts. The Decision Module then uses this integrated textual prompt and enhanced visual input to make action decisions, repeating the cycle until task completion.

and pretrained methods, achieving state-of-the-art zero-shot performance.

REVERIE Complex Task Evaluation In line with the methodology of prior benchmarks (Chen et al. 2024), we evaluate MSNav on the randomly sampled REVERIE subset (70 scenes, 140 samples, named REVERIE-ZS), as shown in Table 3. we used GPT-4o in the Spatial Module for a true zero-shot evaluation, avoiding I-O-S data contamination. MSNav achieves an SR of 45.7% and an SPL of 32.8%, surpassing MapGPT by 4.3% and 4.4%, respectively. This success highlights the Memory Module’s strength in handling REVERIE’s complex, long-range tasks, while the Spatial Module’s object extraction and the viewpoint selection are also contributed. The limited ME improvement is likely due to REVERIE’s rich instructions aiding map construction across all methods.

LLM Spatial Inference Comparison Our evaluation on the I-O-S test set(2720 samples), as shown in Table 4, demonstrates that language models can be effectively trained for spatial reasoning. The fine-tuned Qwen-Sp, with a leading F1 score of 0.316 and an NDCG of 0.388, significantly outperforms a strong one-shot baseline like GPT-4o (+0.046 and +0.063, respectively). This success underscores that targeted fine-tuning is a viable path for imbuing language models with specialized spatial intelligence, present-

	Settings	Methods	SR	SP	OSR	NE
Train		Seq2Seq (Anderson et al. 2018)	21	-	28	7.81
		Speaker (Fried et al. 2018)	35	-	45	6.62
		EnvDrop (Tan, Yu, and Bansal 2019)	52	48	-	5.22
Pretrain		PREVALENT (Hao et al. 2020)	58	53	-	4.71
		RecBERT (Hong et al. 2021b)	63	57	69	3.93
		HAMT (Chen et al. 2021c)	66	61	73	2.29
		DUET (Chen et al. 2022b)	72	60	81	3.31
		LangNav (Pan et al. 2023)	43	-	-	-
		ScaleVLN (Wang et al. 2023)	81	70	88	2.09
		NavCot (Lin et al. 2024)	40	37	48	6.26
		NaviLLM (Zheng et al. 2024)	67	59	-	3.51
		NavGPT-2 _{FlanT5-XL} (Zhou et al. 2024)	68	56	74	3.37
ZS		NavGPT (Zhou, Hong, and Wu 2023)	34	29	42	6.46
		DiscussNav (Long et al. 2023)	43	40	61	5.32
		MapGPT (Chen et al. 2024)	44	35	58	5.63
		MSNav (Ours)	46	40	65	5.24

Table 2: Performance comparison on the complete validation unseen set of the R2R dataset (11 scenes, 783 samples). MSNav achieves the highest SR among all zero-shot methods and surpasses three trained and pretrained approaches.

Settings	Methods	SR	SP	OSR	NE	ME
Train	Seq2Seq (Anderson et al. 2018)	4.2	2.84	8.07	-	-
	Airbert (Guhur et al. 2021)	27.9	21.9	34.5	-	-
	TD-STP (Zhao et al. 2022)	34.9	27.3	39.5	-	-
	SIA (Lin, Li, and Yu 2021)	31.5	16.3	44.7	-	-
	DUET (Chen et al. 2022c)	46.9	33.7	51.0	-	-
ZS	AutoVLN (Chen et al. 2022a)	55.9	40.8	62.1	-	-
	NavGPT (Zhou, Hong, and Wu 2023)	28.9	23.0	32.6	7.86	-
	MapGPT (Chen et al. 2024)	41.4	28.4	56.4	7.12	34.7
	MSNav (Ours)	45.7	32.8	59.3	7.89	35.6

Table 3: Comparison of performance on the REVERIE val unseen dataset. Models in the “Train” setting are evaluated on the full set, while Zero-shot (ZS) models are evaluated on REVERIE-ZS. For a fair comparison, results for NavGPT and MapGPT are our reproductions using GPT-4o.

ing a promising direction for future research. Although the indoor-centric I-O-S dataset currently limits generalization, extending this training approach to more diverse environments, such as outdoor scenes, is a key area for future work.

Model	F1DO \uparrow	F1IO \uparrow	F1 \uparrow	NDCG \uparrow
GPT-4o	0.258	0.150	0.270	0.325
Grok3	0.055	0.057	0.096	0.095
Gemini-2.5-Flash	0.023	0.055	0.096	0.106
Qwen3-4B	0.236	0.039	0.138	0.198
Qwen-Sp (Ours)	0.357	0.179	0.316	0.388

Table 4: Comparative evaluation of object extraction capabilities of different LLMs on the I-O-S test set (2,720 samples). F1DO and F1IO represent the F1 scores for direct and inferred objects, respectively. Qwen-Sp outperforms other models across all metrics.

4.3 Ablation Study

As shown in Table 5, our ablation studies on R2R-ZS confirm the effectiveness of each MSNav module. Notably, removing the Memory Module significantly reduces OSR, which is consistent with its design for improving long-range exploration under oracle stopping conditions. Furthermore, the Spatial Module demonstrates seamless transferability. When integrated into diverse map-based and non-map-based frameworks (e.g., applying its Destination Spatial Layout to NavGPT) via simple prompt modifications, it yields substantial improvements, confirming its effectiveness as a pluggable component.

4.4 Long-Distance Analysis and Efficiency

Performance in Long Distance Tasks On 25 identified long-distance tasks (exceed 10 steps) from the R2R-ZS experiment, MSNav achieved 11 successes versus MapGPT’s 6, increasing the success rate by 20.0% (details in Table 8). The higher success rate of MSNav in long-distance tasks is mainly attributed to the dynamic pruning of the Memory

Module, which discards outdated and irrelevant information, enabling the LLM to focus on the latest data and make accurate judgments under extended trajectories.

Methods	SR \uparrow	SPL \uparrow	OSR \uparrow	NE \downarrow
NavGPT (Zhou, Hong, and Wu 2023)	36.1	31.6	40.3	6.26
NavGPT+Spatial	38.9	34.1	43.1	5.96
MapGPT (Chen et al. 2024)	45.8	37.6	56.5	5.31
MapGPT+Spatial	48.1	39.6	58.3	5.11
MSNav w/o Viewpoint Selection	49.5	41.4	62.5	5.17
MSNav w/o Memory	48.1	40.1	58.8	5.32
MSNav w/o Spatial	47.7	39.6	61.1	5.37
MSNav	50.9	42.6	63.9	5.02

Table 5: Ablation study on R2R-ZS. The table shows the impact of removing MSNav’s modules and the gains from integrating our Spatial Module into other frameworks. For NavGPT, only the Destination Spatial Layout was used.

Method	Steps \downarrow	Length \downarrow	SR \uparrow	SPL \uparrow	OSR \uparrow	NE \downarrow
MapGPT (Chen et al. 2024)	11.84	22.12	24.0	10.0	48.0	10.69
MSNav(Ours)	9.24	15.40	44.0	29.0	60.0	5.41

Table 6: Performance comparison between MapGPT and MSNav on 25 selected challenging long-horizon cases. MSNav demonstrates significant improvements across all key metrics.

Efficiency and Cost Analysis Beyond navigation accuracy, we analyzed MSNav’s computational efficiency. Processing a sample costs \$0.10–\$0.14 and takes 3–5 minutes in our experiments. This is driven by prompt lengths starting at 900–1,000 tokens and growing by 100–250 tokens per step. We consider this a reasonable trade-off for better zero-shot performance. Furthermore, our Memory Module mitigates this cost escalation by dynamically pruning the map, ensuring a manageable prompt size unlike prior methods that accumulate all information.

5 Conclusion

This paper introduces MSNav, a novel zero-shot vision-and-language navigation (ZS-VLN) framework that enhances navigation with dynamic memory, LLM spatial reasoning and LLM-based planning. MSNav demonstrates state-of-the-art performance on the R2R and REVERIE datasets, and its Spatial Module offers versatile plug-and-play integration to augment existing VLN frameworks. To further advance spatial understanding in large models, we introduced the Instruction-Object-Space (I-O-S) dataset. Leveraging this resource, we fine-tuned Qwen3-4B to develop Qwen-Sp, a model that demonstrably surpasses leading commercial LLMs like GPT-4o in critical instruction analysis and object extraction tasks.

References

Anderson, P.; Wu, Q.; Teney, D.; Bruce, J.; Johnson, M.; Sünderhauf, N.; Reid, I.; Gould, S.; and Van Den Hengel, A. 2018. Vision-and-language navigation: Interpreting visually-grounded navigation instructions in real environments. In *Proceedings of the IEEE conference on computer vision and pattern recognition*, 3674–3683.

Baddeley, A. D.; and Hitch, G. 1974. Working memory. In *The Psychology of Learning and Motivation*, volume 8, 47–89. Elsevier.

Brown, T.; Mann, B.; Ryder, N.; Subbiah, M.; Kaplan, J.; Dhariwal, P.; Neelakantan, A.; Shyam, P.; Sastry, G.; Askell, A.; Agarwal, S.; Herbert-Voss, A.; Krueger, G.; Henighan, T.; Child, R.; Ramesh, A.; Ziegler, D. M.; Wu, J.; Winter, C.; Hesse, C.; Chen, M.; Sigler, E.; Litwin, M.; Gray, S.; Chess, B.; Clark, J.; Berner, C.; McCandlish, S.; Radford, A.; Sutskever, I.; and Amodei, D. 2020. Language models are few-shot learners. *Advances in Neural Information Processing Systems*, 33: 1877–1901.

Chang, A.; Dai, A.; Funkhouser, T.; Halber, M.; Nießner, M.; Savva, M.; Song, S.; Zeng, A.; and Zhang, Y. 2017. Matterport3D: Learning from RGB-D data in indoor environments. In *Proceedings of the IEEE International Conference on 3D Vision (3DV)*.

Chen, H.; Suhr, A.; Misra, D.; Snavely, N.; and Artzi, Y. 2019. Touchdown: Natural language navigation and spatial reasoning in visual street environments. In *Proceedings of the IEEE/CVF Conference on Computer Vision and Pattern Recognition*, 12538–12547.

Chen, J.; Lin, B.; Xu, R.; Chai, Z.; Liang, X.; and Wong, K.-Y. K. 2024. MapGPT: Map-Guided Prompting with Adaptive Path Planning for Vision-and-Language Navigation. In *Proceedings of the 62nd Annual Meeting of the Association for Computational Linguistics*.

Chen, K.; Chen, J. K.; Chuang, J.; Vázquez, M.; and Savarese, S. 2021a. Topological Planning with Transformers for Vision-and-Language Navigation. In *Proceedings of the IEEE/CVF Conference on Computer Vision and Pattern Recognition (CVPR)*, 11276–11286.

Chen, S.; Guhur, P.-L.; Schmid, C.; and Laptev, I. 2021b. History Aware Multimodal Transformer for Vision-and-Language Navigation. In *Advances in Neural Information Processing Systems (NeurIPS)*, volume 34, 5834–5847.

Chen, S.; Guhur, P.-L.; Schmid, C.; and Laptev, I. 2021c. History aware multimodal transformer for vision-and-language navigation. *arXiv preprint arXiv:2104.01814*.

Chen, S.; Guhur, P.-L.; Tapaswi, M.; Schmid, C.; and Laptev, I. 2022a. Learning from Unlabeled 3D Environments for Vision-and-Language Navigation. *arXiv:2208.11781*.

Chen, S.; Guhur, P.-L.; Tapaswi, M.; Schmid, C.; and Laptev, I. 2022b. Think Global, Act Local: Dual-scale Graph Transformer for Vision-and-Language Navigation. In *Proceedings of the IEEE/CVF Conference on Computer Vision and Pattern Recognition (CVPR)*, 16537–16547.

Chen, S.; Guhur, P.-L.; Tapaswi, M.; Schmid, C.; and Laptev, I. 2022c. Think Global, Act Local: Dual-scale Graph Transformer for Vision-and-Language Navigation. *arXiv:2202.11742*.

Chen, Y.-C.; Li, L.; Yu, L.; El Kholy, A.; Ahmed, F.; Gan, Z.; Cheng, Y.; and Liu, J. 2020. Uniter: Universal image-text representation learning. In *European Conference on Computer Vision*, 104–120. Springer.

Cheng, T.; Song, L.; Ge, Y.; Liu, W.; Wang, X.; and Shan, Y. 2024. YOLO-World: Real-Time Open-Vocabulary Object Detection. *arXiv preprint arXiv:2401.17270*.

Deng, Z.; Narasimhan, K.; and Russakovsky, O. 2020. Evolving graphical planner: Contextual global planning for vision-and-language navigation. *Advances in Neural Information Processing Systems*, 33: 20660–20672.

Epstein, R. A.; Patai, E. Z.; Julian, J. B.; and Spiers, H. J. 2017. The cognitive map in humans: spatial navigation and beyond. *Nature Neuroscience*, 20(11): 1504–1513.

Fried, D.; Hu, R.; Cirik, V.; Rohrbach, A.; Andreas, J.; Morency, L.-P.; Berg-Kirkpatrick, T.; Saenko, K.; Klein, D.; and Darrell, T. 2018. Speaker-follower models for vision-and-language navigation. *Advances in Neural Information Processing Systems*, 31.

Fuentes-Pacheco, J.; Ruiz-Ascencio, J.; and Rendon-Mancha, J. M. 2015. Visual simultaneous localization and mapping: A survey. *Artificial Intelligence Review*, 43: 55–81.

Google DeepMind. 2025. Start Building with Gemini 2.5 Flash. <https://developers.googleblog.com/en/start-building-with-gemini-25-flash/>. Accessed: 2025-05-19.

Guhur, P.-L.; Tapaswi, M.; Chen, S.; Laptev, I.; and Schmid, C. 2021. Airbert: In-domain Pretraining for Vision-and-Language Navigation. *arXiv:2108.09105*.

Hao, W.; Li, C.; Li, X.; Carin, L.; and Gao, J. 2020. Towards learning a generic agent for vision-and-language navigation via pre-training. In *Proceedings of the IEEE/CVF Conference on Computer Vision and Pattern Recognition*, 13137–13146.

Hong, Y.; Wu, Q.; Qi, Y.; Rodriguez-Opazo, C.; and Gould, S. 2021a. VLN BERT: A Recurrent Vision-and-Language BERT for Navigation. In *Proceedings of the IEEE/CVF Conference on Computer Vision and Pattern Recognition (CVPR)*, 1643–1653.

Hong, Y.; Wu, Q.; Qi, Y.; Rodriguez-Opazo, C.; and Gould, S. 2021b. VLN BERT: A Recurrent Vision-and-Language BERT for Navigation. In *Proceedings of the IEEE/CVF Conference on Computer Vision and Pattern Recognition (CVPR)*, 1643–1653.

Hu, E. J.; Shen, Y.; Wallis, P.; Allen-Zhu, Z.; Li, Y.; Wang, S.; Wang, L.; and Chen, W. 2022. LoRA: Low-Rank Adaptation of Large Language Models. In *Proceedings of the International Conference on Learning Representations (ICLR)*.

Huang, H.; Jain, V.; Mehta, H.; Ku, A.; Magalhaes, G.; Baldridge, J.; and Ie, E. 2019. Transferable Representation Learning in Vision-and-Language Navigation. In *Proceedings of the IEEE/CVF International Conference on Computer Vision (ICCV)*, 7403–7412. IEEE.

Ke, L.; Li, X.; Bisk, Y.; Holtzman, A.; Gan, Z.; Liu, J.; Gao, J.; Choi, Y.; and Srinivasa, S. 2019. Tactical Rewind: Self-Correction via Backtracking in Vision-and-Language Navigation. In *Proceedings of the IEEE/CVF Conference on Computer Vision and Pattern Recognition (CVPR)*, 6741–6749. IEEE.

Kojima, T.; Gu, S. S.; Reid, M.; Matsuo, Y.; and Iwasawa, Y. 2022. Large Language Models are Zero-Shot Reasoners. *arXiv preprint arXiv:2205.11191*.

Krantz, J.; Wijmans, E.; Majumdar, A.; Batra, D.; and Lee, S. 2020. Beyond the nav-graph: Vision-and-language navigation in continuous environments. In *European Conference on Computer Vision*, 104–120. Springer.

Li, X.; Yin, X.; Li, C. Y.; Zhang, P.; Hu, X.; Zhang, L.; Wang, L.; Hu, H.; Dong, L.; Wei, F.; Choi, Y.; and Gao, J. 2020. Oscar: Object-Semantics Aligned Pre-training for Vision-Language Tasks. In *Proceedings of the European Conference on Computer Vision (ECCV)*, 121–137. Springer.

Lin, B.; Nie, Y.; Wei, Z.; Chen, J.; Ma, S.; Han, J.; Xu, H.; Chang, X.; and Liang, X. 2024. NavCoT: Boosting LLM-Based Vision-and-Language Navigation via Learning Disentangled Reasoning. *arXiv preprint arXiv:2403.07376*.

Lin, X.; Li, G.; and Yu, Y. 2021. Scene-Intuitive Agent for Remote Embodied Visual Grounding. *arXiv:2103.12944*.

Long, Y.; Li, X.; Cai, W.; and Dong, H. 2023. Discuss Before Moving: Visual Language Navigation via Multi-expert Discussions. *arXiv preprint arXiv:2309.11382*.

Ma, C.-Y.; Wu, Z.; AlRegib, G.; Xiong, C.; and Kira, Z. 2019. The Regretful Agent: Heuristic-Aided Navigation Through Progress Estimation. In *Proceedings of the IEEE/CVF Conference on Computer Vision and Pattern Recognition (CVPR)*, 6732–6740.

Malleret, G.; Salin, P.; Mazza, S.; and Plancher, G. 2024. Working memory forgetting: Bridging gaps between human and animal studies. *Neuroscience & Biobehavioral Reviews*, 163: 105742.

OpenAI. 2023. GPT-4 Technical Report. *arXiv preprint arXiv:2303.08774*.

OpenAI. 2024. GPT-4o System Card. <https://arxiv.org/abs/2410.21276>. Accessed: 2025-05-19.

Pan, B.; Panda, R.; Jin, S.; Feris, R.; Oliva, A.; Isola, P.; and Kim, Y. 2023. LangNav: Language as a Perceptual Representation for Navigation. *arXiv preprint arXiv:2310.07889*.

Qi, Y.; Wu, Q.; Anderson, P.; Wang, X.; Wang, W. Y.; Shen, C.; and Hengel, A. v. d. 2020. Reverie: Remote embodied visual referring expression in real indoor environments. In *Proceedings of the IEEE/CVF Conference on Computer Vision and Pattern Recognition*, 9982–9991.

Skaramagkas, V.; Giannakakis, G.; Ktistakis, E.; Manousos, D.; Karatzanis, I.; Tachos, N. S.; Tripoliti, E.; Marias, K.; Fotiadis, D. I.; and Tsiknakis, M. 2023. Review of Eye Tracking Metrics Involved in Emotional and Cognitive Processes. *IEEE Reviews in Biomedical Engineering*, 16: 260–277.

Tan, H.; Yu, L.; and Bansal, M. 2019. Learning to Navigate Unseen Environments: Back Translation with Environmental Dropout. 2610–2621. Minneapolis, Minnesota.

Thrun, S. 1998. Learning metric-topological maps for indoor mobile robot navigation. *Artificial Intelligence*, 99(1): 21–71.

Wang, X.; Huang, Q.; Celikyilmaz, A.; Gao, J.; Shen, D.; Wang, Y.-F.; Wang, W. Y.; and Zhang, L. 2019. Reinforced Cross-Modal Matching and Self-Supervised Imitation Learning for Vision-Language Navigation. In *Proceedings of the IEEE/CVF Conference on Computer Vision and Pattern Recognition (CVPR)*, 6630–6639. IEEE.

Wang, Z.; Li, J.; Hong, Y.; Wang, Y.; Wu, Q.; Bansal, M.; Gould, S.; Tan, H.; and Qiao, Y. 2023. Scaling data generation in vision-and-language navigation. In *Proceedings of the IEEE/CVF International Conference on Computer Vision*, 12009–12020.

Wei, J.; Wang, X.; Schuurmans, D.; Bosma, M.; Ichter, B.; Xia, F.; Chi, E.; Le, Q.; and Zhou, D. 2022. Chain-of-thought prompting elicits reasoning in large language models. *Advances in Neural Information Processing Systems*, 35: 24824–24837.

xAI. 2025. Grok 3 Beta — The Age of Reasoning Agents. Accessed: 2025-05-19.

Yang, A.; Li, A.; Yang, B.; Zhang, B.; Hui, B.; Zheng, B.; Yu, B.; Gao, C.; Huang, C.; Lv, C.; Zheng, C.; Liu, D.; Zhou, F.; Huang, F.; Hu, F.; Ge, H.; Wei, H.; Lin, H.; Tang, J.; Yang, J.; Tu, J.; Zhang, J.; Yang, J.; Yang, J.; Zhou, J.; Zhou, J.; Lin, J.; Dang, K.; Bao, K.; Yang, K.; Yu, L.; Deng, L.; Li, M.; Xue, M.; Li, M.; Zhang, P.; Wang, P.; Zhu, Q.; Men, R.; Gao, R.; Liu, S.; Luo, S.; Li, T.; Tang, T.; Yin, W.; Ren, X.; Wang, X.; Zhang, X.; Ren, X.; Fan, Y.; Su, Y.; Zhang, Y.; Zhang, Y.; Wan, Y.; Liu, Y.; Wang, Z.; Cui, Z.; Zhang, Z.; Zhou, Z.; and Qiu, Z. 2025. Qwen3 Technical Report. In *arXiv preprint arXiv:2505.09388*.

Yao, S.; Zhao, J.; Yu, D.; Du, N.; Shafran, I.; Narasimhan, K.; and Cao, Y. 2022. React: Synergizing reasoning and acting in language models. *arXiv preprint arXiv:2210.03629*.

Zhao, Y.; Chen, J.; Gao, C.; Wang, W.; Yang, L.; Ren, H.; Xia, H.; and Liu, S. 2022. Target-Driven Structured Transformer Planner for Vision-Language Navigation. *arXiv:2207.11201*.

Zheng, D.; Huang, S.; Zhao, L.; Zhong, Y.; and Wang, L. 2024. Towards Learning a Generalist Model for Embodied Navigation. *arXiv:2312.02010*.

Zhou, G.; Hong, Y.; Wang, Z.; Wang, X. E.; and Wu, Q. 2024. NavGPT-2: Unleashing Navigational Reasoning Capability for Large Vision-Language Models. *arXiv:2407.12366*.

Zhou, G.; Hong, Y.; and Wu, Q. 2023. NavGPT: Explicit Reasoning in Vision-and-Language Navigation with Large Language Models. *arXiv preprint arXiv:2305.16986*.

A Experiment Details

A.1 Analysis of MSNav Potential with Multi Round Experiment

While MSNav demonstrates strong zero-shot performance, we further conducted an exploratory analysis to estimate its potential upper bound. This iterative refinement process, with round-by-round results detailed in Table 7, showed that by cumulatively refining performance—in each round, we re-evaluated samples that had failed in the previous round’s cumulative results, and then updated the overall results with these new outcomes—MSNav’s SR could be significantly enhanced. This process was halted after five rounds because the improvement in Oracle Success Rate (OSR) became marginal (increasing from 76.4% in the fourth round to 77.8% in the fifth round). This saturation suggested that the remaining failures were largely due to episodes where the target was fundamentally unreachable by the agent, rather than sub-optimal local decisions. Through this iterative refinement, MSNav’s SR was progressively improved from its initial 50.9% to a remarkable 73.6%, with a corresponding increase in SPL from 42.6% to 59.3%.

This significant gap primarily highlights the current variability and sub-optimality in the LLM’s decision-making process for VLN tasks. While strategies such as reducing LLM temperature can enhance output consistency, they often bias the agent towards overly conservative actions (e.g., premature STOP decisions), which can be detrimental, particularly in long-horizon navigation tasks. Nevertheless, achieving a 73.6% SR through the described iterative refinement—a figure that surpasses many fully supervised or pretrained methods—underscores the immense, albeit not fully realized, potential of LLMs in this domain. This strongly suggests that future efforts focused on optimizing the LLM’s output for navigational decision-making are crucial for substantially advancing the performance of LLM-based ZS-VLN systems like MSNav.

A.2 MSNav’s Performance in Long Distance Tasks

In the 216 cases of the R2R-ZS, MapGPT had 25 cases where the number of steps exceeded 10. Among them, only 6 cases were successful, with a success rate of 24.0%. In contrast, MSNav achieved 11 successes among these 25 cases, with a success rate increase of 20.0%. The detailed indicators are shown in the Table 8. The higher success rate of MSNav in long-distance tasks is mainly attributed to the dynamic pruning of the Memory Module, which discards outdated and irrelevant information, enabling the LLM to focus on the latest data and make accurate judgments under extended trajectories. However, it is undeniable that the spatial reasoning and visual enhancement capabilities of the Spatial Module have continuously made positive contributions to the higher success rate of MSNav.

A.3 Memory Module Details

The Memory Module module’s dynamic map pruning, described in Memory Module Section, uses optimized parameters to maintain a compact topological map. The parameters

Iteration Round	SR \uparrow	SPL \uparrow	OSR \uparrow	NE \downarrow
1 (Base MSNav)	50.9	42.6	63.9	5.02
2	62.5	51.3	70.8	4.46
3	67.1	54.3	74.5	4.31
4	69.9	56.2	76.4	4.05
5	73.6	59.3	77.8	3.67

Table 7: MSNav performance progression on the R2R-ZS with 5 iterative rounds. Each round addresses failures from the preceding one.

Method	Steps \downarrow	Length \downarrow	SR \uparrow	SPL \uparrow	OSR \uparrow	NE \downarrow
MapGPT	11.84	22.12	24.0	10.0	48.0	10.69
MSNav	9.24	15.40	44.0	29.0	60.0	5.41

Table 8: Performance comparison between MapGPT and MSNav on 25 selected challenging long-horizon cases. MSNav demonstrates significant improvements across all key metrics.

include $t_{\text{start}} = 15$, $\theta_{\text{recent-visit}} = 3$, $\theta_{\text{age}} = 10$, $N_{\text{remove}} = 1$, $\lambda_t = 1.0$, $\lambda_d = 2.0$, $\lambda_f = 5.0$, and $\lambda_{\text{dist}} = 0.5$. These values, tuned empirically via grid search on the R2R subset (Anderson et al. 2018), balance map compactness and navigation efficiency. We gradually analyzed the node pruning behavior of the Memory Module to select reasonable hyperparameters instead of performing traditional hyperparameter search over the entire dataset to maximize the success rate. Specifically, we relied on qualitative observations of a single scenario to select the appropriate parameter combination. Validated on R2R and REVERIE (Qi et al. 2020), these settings achieved ME scores of 40.4% and 35.6%, respectively.

A.4 Metric Details

This section provides definitions for all evaluation metrics used in the experiments to ensure clarity and reproducibility. Standard VLN metrics (NE, SR, OSR, SPL) follow established definitions (Anderson et al. 2018), while F1 and NDCG are tailored to the I-O-S dataset’s object extraction task. The novel Map Efficiency (ME) metric is detailed to highlight its role in evaluating topological map quality.

Navigation Error (NE) NE measures the average Euclidean distance (in meters) between the agent’s final position and the target location at the end of an episode.

Success Rate (SR) SR is the percentage of episodes where the agent stops within 3 meters of the target location.

Oracle Success Rate (OSR) OSR is the percentage of episodes where the agent passes within 3 meters of the target at any point during navigation, assuming an oracle stop policy.

Success weighted by Path Length (SPL) SPL balances navigation success and path efficiency, computed as the ratio of the shortest path length to the actual path length, weighted by success.

F1 Score The F1 score measures the precision and recall of extracted object lists in the I-O-S dataset. It is computed

separately for direct objects (F1DO, objects explicitly mentioned in instructions) and inferred objects (F1IO, objects implicitly relevant based on context). The overall F1 score is calculated for the entire object list, which combines both direct and inferred objects into a single set.

Normalized Discounted Cumulative Gain (NDCG)

NDCG assesses the ranking quality of extracted objects by comparing the predicted object list to the ground-truth list. It accounts for the relevance order of objects, with higher scores indicating better alignment with the ground-truth ranking. For each sample, NDCG is calculated as:

$$\text{NDCG} = \frac{\text{DCG}}{\text{IDCG}}, \quad (5)$$

where DCG is the discounted cumulative gain based on predicted object ranks, and IDCG is the ideal DCG based on the ground-truth ranks.

Map Efficiency (ME) The Map Efficiency (ME) metric evaluates the quality of topological maps in VLN tasks. It is defined as:

$$\text{ME} = \frac{|T_t \cap T_{\text{expert}}|}{|T_{\text{expert}}|} \cdot \frac{1}{1 + \alpha \cdot \frac{|V_t|}{|T_{\text{expert}}|}}, \quad (6)$$

where T_t represents the agent’s trajectory, T_{expert} denotes the expert path node set, V_t is the agent’s map node set, and $\alpha = 0.25$. The first term quantifies the proportion of expert nodes covered by the trajectory, while the second term penalizes overly large maps. A higher ME score indicates a more compact and efficient map. MSNav’s Memory Module pruning strategy yields superior ME scores, demonstrating enhanced map efficiency. The penalty factor $\alpha = 0.25$ was optimized through a grid search over the range [0.1, 1.0] using the R2R subset.

A.5 Qwen-Sp Fine-tuning Details

This study employs the pretrained Qwen3-4B, a causal language model with approximately 4 billion parameters, as the base model. To adapt it for instruction-following and scene understanding tasks in vision-language navigation (VLN), we utilize Low-Rank Adaptation (LoRA), a parameter-efficient fine-tuning (PEFT) technique. Specifically, we train two independent LoRA adapters on the I-O-S dataset, comprising 25,694 training samples: the Object Adapter, which predicts task-relevant object pairs from instructions, and the Spatial Relation Adapter, which infers spatial relationships and overall layouts among objects.

To ensure consistency and comparability, both adapters share the same LoRA configuration. The rank of the low-rank matrices is set to $r = 16$, the scaling factor to $\alpha = 32$, and the dropout rate for LoRA layers to 0.05. The LoRA adapters are applied to key layers of the Qwen3 model, specifically the projection layers of the multi-head self-attention (MHSA) mechanism—namely, the query (q_{proj}), key (k_{proj}), value (v_{proj}), and output (o_{proj}) projections—as well as the linear layers of the feed-forward network (FFN), comprising the gate ($gate_{\text{proj}}$), up (up_{proj}), and down ($down_{\text{proj}}$) projections in the SwiGLU-based FFN. These layers are selected due to their critical role in instruction

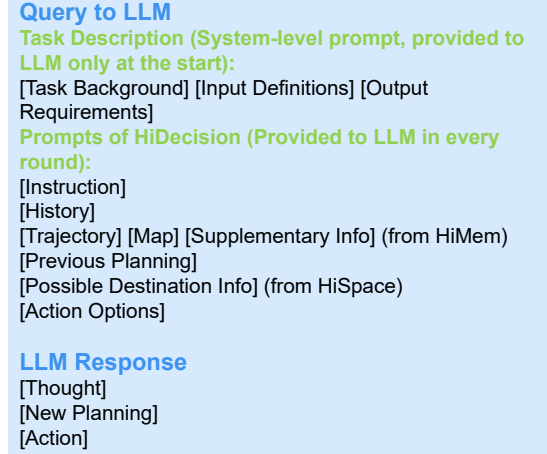


Figure 5: Complete prompt structure. The top section specifies the static system-level task description prompt provided to the LLM at the outset. The middle section elaborates on the dynamic prompts supplied during each navigation round. The bottom section presents the LLM’s response.

understanding, as MHSA layers effectively model complex dependencies within text sequences, and FFN layers enable nonlinear transformations and high-level feature abstraction. This targeted application of LoRA facilitates efficient learning of task-specific patterns while minimizing computational and storage requirements.

The fine-tuning process employs the AdamW optimizer in PyTorch, with an initial learning rate of 1×10^{-4} , a cosine decay schedule, and a weight decay of 0.1 for L2 regularization. The maximum gradient norm is clipped at 1.0, and training is performed using bfloat16 (bf16) mixed precision without gradient accumulation. The Object Adapter is trained for 1 epoch with a per-device batch size of 64, while the Spatial Relation Adapter is trained for 8 epochs with a per-device batch size of 48.

B Prompt Structures

ZS-VLN Prompts This section describes the prompt structures employed by MSNav to guide the LLM in ZS-VLN tasks. The overall prompt architecture is depicted in Figure 5. The task description prompt is elaborated in Figure 6, while the single-round prompt input to the HiDecision module is shown in Figure 7. For experiments on the REVERIE dataset, only the instruction component is modified to:

“Instruction’ serves as global guidance that you should follow. Your task is to locate the specified or hidden target object, stop, and disregard any actions related to the target object mentioned in the ‘Instruction’. You should not overly focus on color details of landmarks or the target object described in the ‘In-

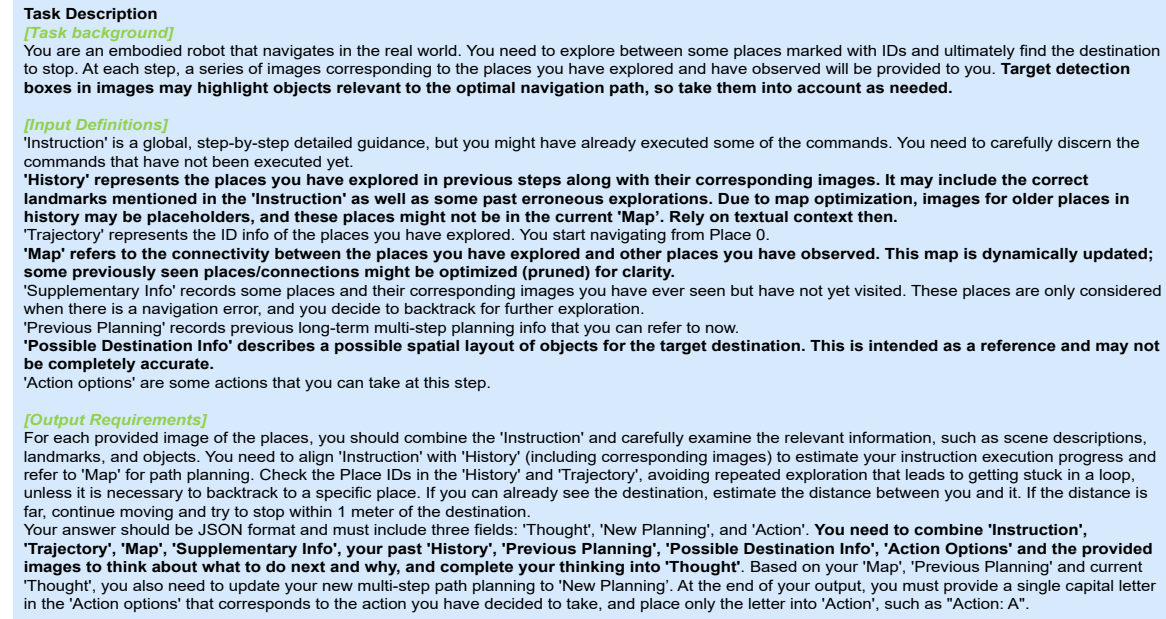


Figure 6: Task description prompts for the R2R dataset. The bolded sections in the figure highlight the prompt representations of each MSNav module. For the REVERIE dataset, only the instruction section was modified, while the other sections remained unchanged.

struction', as these color descriptions may be inaccurate."

All other components remain consistent with those used for the R2R dataset. Our prompt design draws on insights from prior work (Chen et al. 2024) while incorporating adaptations tailored to MSNav's framework.

Spatial Inferring Prompts To evaluate the spatial imagination and reasoning capabilities of leading commercial large language models (LLMs), we utilize the prompt shown in Figure 9 to evaluate their ability to extract objects from instructions. For experiments on the REVERIE dataset, to ensure a zero-shot setting, we refrain from using our Qwen-Sp model. Instead, we employ GPT-4o for extracting the object list and predicting the destination spatial layout. The corresponding prompts are presented in Figures 9 and 10, respectively.

C Details of Viewpoint Selection

The viewpoint selection process begins by checking a cache for pre-computed candidates at the agent's current physical location, identified by its scan and viewpoint ID. If this location is visited for the first time, an exploration phase is initiated. The system simulates a full 360-degree panoramic observation by rotating the agent's camera through 36 discrete views covering all directions. During this scan, all adjacent navigable viewpoints are identified and aggregated into a preliminary list. For each potential destination, the system records its location, the initial camera angle from which it was discovered, and its 3D coordi-

nates. This initial discovery ensures all reachable neighbors are considered before any optimization occurs.

Following the discovery phase, the process optimizes the representative view for each candidate to ensure it is maximally informative. For every identified candidate, the algorithm calculates the precise 3D direction vector from the agent's current position to the candidate's location. This ideal vector is then mapped to the closest of the 36 discrete camera angles available to the agent. The candidate's associated data, particularly its representative image and view index, is updated to reflect this new, optimized viewing direction, which points more directly at the target. This refined list of candidates, each with an optimal representative view, is then stored in the cache to accelerate future visits and is returned to the agent to inform its next navigation decision.

D Qualitative Analysis of MSNav

D.1 Successful Case Study

This successful case demonstrates that the MSNav framework effectively tackles complex instruction-guided navigation problems for challenging pathfinding tasks. It achieves this by integrating several key capabilities: Memory Module's dynamic pruning, Spatial Module's spatial relationship information, and its own visual enhancement.

Consider the instruction: "Walk down the stairs all the way and past the Christmas tree. Make a right turn and walk past the blue chair into the room with the white sink." This instruction delineates transitions across three key locations: the stairs, the room with the blue chair, and the room

Query to LLM

Instruction
Turn left and to towards the kitchen, turn left at the kitchen and go until you are right before the yellow couch by the picture on your right.

History
step 0: turn left to Place 2 which is corresponding to Image 2, step 1: turn left to Place 3 which is corresponding to Image 3, step 2: go forward to Place 6 which is corresponding to Image 6, step 3: go forward to Place 8 which is corresponding to Image 8

Trajectory
Place 0 2 3 6 8

Map
Place 0 is connected with Places 1, 2
Place 2 is connected with Places 0, 3, 4, 5
Place 3 is connected with Places 1, 6, 7, 2
Place 6 is connected with Places 1, 8, 9, 7, 3
Place 8 is connected with Places 10, 11, 9, 6

Supplementary Info
Place 1, which is corresponding to Image 1
Place 4, which is corresponding to Image 4
Place 5, which is corresponding to Image 5
Place 7, which is corresponding to Image 7

Previous Planning
1. Go forward to Place 8.
2. Stop before the yellow couch by the picture.

Possible Destination Info (For reference only, may not be completely accurate)
The destination is the living room, located near a couch. The spatial layout of the destination is centered around a couch with a pillow, with a picture nearby and a bench also in the vicinity.

Action Options (step 4)
['A. stop', 'B. go forward to Place 10 which is corresponding to Image 10', 'C. turn right to Place 11 which is corresponding to Image 11', 'D. turn right to Place 9 which is corresponding to Image 9', 'E. turn around to Place 6 which is corresponding to Image 6']

LLM Response

Thought
I am currently at Place 8, which corresponds to Image 8. The instruction is to stop right before the yellow couch by the picture on the right. Image 8 shows a living room with a sofa and a picture, but no yellow couch is visible. **The Possible Destination Info suggests the destination is near a couch with a picture nearby. I should explore further to find the yellow couch and picture.**

New Planning
1. Turn right to Place 11 to check for the yellow couch and picture. 2. If not found, explore Place 9."

Action: "C"

Figure 7: Prompt input to the Decision Module for a specific example in a single navigation round. The bolded sections highlight the contributions of MSNav’s modules, with the Map and Supplementary Info components dynamically updated based on pruning. The LLM Response’s thought section demonstrates the influence of Possible Destination Info, showing how the LLM incorporates the provided destination description into its decision-making process.

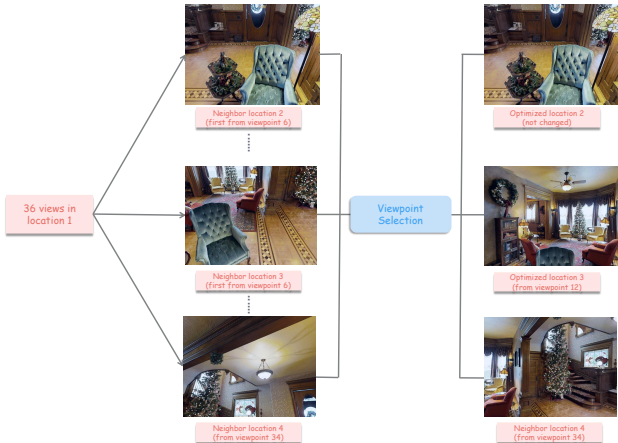


Figure 8: Illustration of the representative view optimization. The candidate viewpoint of neighbor location is initially discovered. Then select the optimized view which directly faces the target to represent this candidate.

with the white sink. Spatial Module provides MSNav with potential destination information, including a detailed linguistic description of the final destination extracted from the instruction and the spatial relationships of objects surrounding it. Meanwhile, Spatial Module enhances the visual scene images by highlighting object pairs inferred by Qwen-SP, marking existing objects in green (as shown in Figures 11, 12, and 13). These enhanced images are then fed into MSNav.

After step 15, MSNav activates Memory Module’s dynamic pruning mechanism. In each subsequent step, it calculates a “pruning priority score” for trajectory points meeting specific criteria and removes the point with the highest score. As illustrated in the figures, at step 15, the point with the highest pruning priority score is “forgotten” (removed from the map) based on the calculated scores. This process eliminates trajectory points irrelevant to the current decision, thereby increasing the likelihood of progressing toward the final destination. In every subsequent decision step, MSNav continues this dynamic pruning, retaining only those trajectory points likely to lead to the final destination. This iterative process, akin to human pathfinding, enables robust and successful navigation in complex environments.

D.2 Failed Case Study

This case illustrates a failure in instruction-following navigation, with the instruction: “Turn right to exit the room. Turn right when you reach the end of the hallway. Walk to-

ward the couches and stop there by the couches.” The instruction outlines clear sequential sub-goals: (1) exit the current room, (2) turn right at the end of the hallway, and (3) walk toward the couches and stop nearby.

The agent successfully completed the first sub-goal in Step 0 (moving from Place 0 to Place 3), correctly turning right to exit the room. However, the failure occurred during the execution of the second sub-goal, which required the agent to “turn right when you reach the end of the hallway.” After reaching Place 3 in Step 0, the agent proceeded to “go forward to Place 6” in Step 1. Critically, upon arriving at Place 6, the agent failed to execute the required second “right turn” as specified. Instead, in Step 2 (moving from Place 6 to Place 8), it performed a “left turn to Place 8,” as depicted in Figure 14. Relying on the “Possible Destination Info,” which provided clues about the couches (Place 8 contains a sofa chair and side table), the agent incorrectly identified Place 8 as the destination and executed the stop action. Consequently, it failed to complete the full navigation path and all intermediate steps, as shown in Figure 15.

The agent appears to have over-prioritized reaching a location matching the final destination’s description, stopping prematurely after mistakenly assuming it had completed all necessary intermediate navigation steps.

E I-O-S Dataset Details

The Instruction-Object-Space (I-O-S) dataset is designed to enhance spatial reasoning in vision-and-language navigation (VLN) by integrating natural language instructions, task-relevant objects, and their spatial configurations. The dataset contains 28,414 samples, with 25,694 allocated for training and 2,720 for testing. These samples are derived from oracle paths in the REVERIE dataset (Qi et al. 2020) and manually crafted trajectories developed for this study. Each sample consists of a natural language instruction I , a list of relevant objects O , and the spatial arrangement at the destination S . The average instruction length is 23.05 words. Object lists are categorized into direct and inferred objects, with averages of 3.99 and 9.98 objects, respectively. Descriptions of the spatial layout at the destination have an average length of 39.12 words. An example from the I-O-S dataset is provided below:

- **Instruction:** Exit the kitchen area through the doorway slightly to your left. Walk across the dining table area. Turn right and pass the blue chair or sofa near the Christmas tree. Stop there.
- **Direct Objects:** [“chair”, “sofa chair”, “table”, “Christmas tree”]
- **Inferred Objects:** [“mirror”, “lamp”, “plant”, “picture”, “painting”, “decoration”, “fan”, “light”, “island”, “heater”, “trash can”, “stool”, “cabinet”, “coffee table”]
- **Destination Spatial Layout:** “The destination is the foyer or entryway, located near a blue chair and a Christmas tree. The spatial layout includes a blue chair or sofa positioned beside a Christmas tree, with a coffee table and a lamp also present in the area.”

To construct the I-O-S dataset, we processed data from the REVERIE dataset and our manually annotated trajectories as follows. For samples derived from REVERIE, we directly used its pre-generated bounding box files, which contains object IDs, names, visible view indices, and bounding boxes in $[x, y, w, h]$ format. For our custom instructions and trajectories, we adopted the REVERIE methodology (Qi et al. 2020) to generate bounding boxes by (1) using Matterport3D’s 3D object annotations (center point, axis directions, radii) to define object vertices, (2) projecting these vertices onto 2D image planes using viewpoint camera poses to form $[x, y, w, h]$ bounding boxes, (3) filtering occluded objects by comparing depth overlaps with closer objects, and (4) including only objects within 3 meters of the viewpoint. These annotations are stored in JSON files matching REVERIE’s format for consistency.

After obtaining the objects observed along the expert trajectories (i.e., the bounding box files for each navigation point), we processed them as follows to derive the corresponding object lists and destination spatial layouts. For each navigation point, we prompt LLM Gemini-2.5-Flash to select and classify “direct objects” (those explicitly mentioned in the instructions) and “potential objects” (those present in the object list but not mentioned in the instructions) based on the bounding box coordinates of the ground-truth objects in each view and their relevance to the instructions. The layout of the final destination is predicted by combining the spatial cues derived from the instructions with the lists of direct and potential objects and their bounding box coordinates. After the LLM completed the prediction, in order to minimize the cost of dataset generation, we adopted an iterative LLM prompt engineering and quality control process to ensure the quality of the prediction. We randomly selected a subset of I-O-S for quality assessment. We compared the descriptions and lists generated by the LLM with the corresponding scene screenshots to ensure semantic accuracy. After each verification, we analyzed the errors and improved the LLM prompt, and repeated this process with new samples until the sampled data reached the high-quality standards in terms of spatial reasoning and object prediction.

The final destination’s spatial layout is described using natural language. Although it was verified through the ground-truth object list and its bbox coordinates, due to the hallucination problem of LLM, it cannot be completely avoided, which may have a negative impact on task completion. To alleviate this situation, our system prompts explicitly: “The ‘possible destination information’ describes the possible object spatial layout of the target destination. This is for reference only and may not be completely accurate.” Unlike object list extraction, which uses direct metrics, spatial layout assessment currently relies on indirect validation through VLN task performance, highlighting the need for dedicated metrics for a more direct and streamlined evaluation of this capability.

Objective

- Add two new fields to each JSON entry: `direct_obj` and `potential_obj`, based on the instruction field.
 - `direct_obj`: A list of all objects explicitly mentioned in instruction (e.g., `["sink", "table"]` in "clean the sink and table").
 - `potential_obj`: A list of objects reasonably inferred based on the task or room type, describing the environment or related to the task.
- Retain original fields (`instruction`) unchanged in the output.

Processing Steps

Identify Direct Object (`direct_obj`)

- Extract all objects explicitly named in instruction as targets of the main task or verbs.
 - Focus on nouns syntactically tied to task-related verbs (e.g., "sink" and "table" in "clean the sink and table").
 - Use syntactic parsing (e.g., dependency parsing) to identify direct objects of verbs when possible.
 - Include all objects explicitly mentioned as task targets, even if tied to different verbs (e.g., "clean the sink and organize the table" → `["sink", "table"]`).
- Sort `direct_obj` using:
 1. Frequency (40%): Objects mentioned multiple times rank higher.
 2. Task Relevance (40%): Objects tied to the primary task or verb rank higher (e.g., "sink" in "clean the sink and check the table").
 3. Order of Mention (20%): Earlier-mentioned objects rank higher if frequency and relevance are equal.
- If no objects are mentioned (e.g., "go to the spa") or only pronouns/vague terms are used (e.g., "clean it"), set `direct_obj` to `[]`.
- Match nouns exactly as in instruction (e.g., "sink", not "basin").
- Do not infer objects for `direct_obj`; they must be explicitly stated.

Identify Potential Objects (`potential_obj`)

- Include objects that are:
 - Inferred based on the task or room type, up to a maximum of 3 inferred objects (5 for vague instructions), describing the environment or context (e.g., "bed", "tiles" in "Go to the spa with one bed, brown tiles").
 - Guidelines for inference:
 - Select inferred objects most relevant to the task (e.g., "sponge" for cleaning) or room type (e.g., "towel" in a spa).
 - Avoid speculative inferences (e.g., do not infer "chandelier" in a spa unless mentioned).
 - Use singular nouns for inferred objects unless context suggests plural.
 - If more than 3 (or 5 for vague instructions) inferred objects are possible, prioritize by typicality (e.g., "sponge" over "toaster" for cleaning in a kitchen).
- Sort `potential_obj` by:
 1. Explicit Mention (40%): Explicitly mentioned objects rank higher.
 2. Frequency (30%): Objects mentioned multiple times rank higher.
 3. Task Relevance (30%): Objects closer to the task or central to the environment rank higher (e.g., "sponge" for cleaning over "lamp").
- If no objects are inferred, set `potential_obj` to `[]`.

Handle Special Cases

- Vague Instructions:
 - An instruction is vague if it lacks specific object nouns (e.g., "clean the room") or uses generic verbs without clear targets (e.g., "fix something").
 - Set `direct_obj` to `[]` and infer up to 5 typical objects for `potential_obj` based on room type (e.g., `["table", "chair", "lamp"]` for a generic room).
- Compound Objects:
 - Include all explicitly mentioned task targets in `direct_obj` (e.g., "clean the sink and table" → `["sink", "table"]`), sorted as above.
- Non-Physical Objects:
 - Exclude abstract entities (e.g., "mess" in "clean the mess") from both `direct_obj` and `potential_obj`, setting to `[]`.
 - Allow inferred physical objects relevant to the task (e.g., "sponge" for cleaning).
- Multi-Room Instructions:
 - Infer `potential_obj` based on the room where the task occurs (e.g., spa for "go from kitchen to spa and clean the sink"). If unclear, use the last-mentioned room.
- Empty/Malformed Instructions:
 - If instruction is empty, null, or malformed (e.g., ""), set `direct_obj` to `[]` and `potential_obj` to `[]`.

Input Validation

- Validate input JSON before processing:
 - If instruction is missing, set `direct_obj` to `[]` and `potential_obj` to `[]`.
 - If other required fields (path, heading, scan, path_id, instr_id) are missing, retain them as null or their default type (e.g., empty list for path) and proceed.

Output Format

- Generate a JSON dictionary with fields in order: `instruction`, `direct_obj`, `potential_obj`.
- Ensure:
 - `direct_obj` is a list of strings, sorted by frequency, task relevance, order of mention, and alphabetical tiebreaker.
 - `potential_obj` is a list of strings, sorted by explicit mention, frequency, task relevance, and alphabetical tiebreaker.
 - JSON is well-formed, with 2-space indentation, no trailing commas, and consistent double quotes.
 - Original fields (`instruction`) are unchanged.
- Validate output:
 - All required fields are present in the specified order.
 - `direct_obj` and `potential_obj` are lists of strings.
 - JSON syntax is correct with no trailing commas or missing brackets.

Notes

- Exact Matching for `direct_obj`: Match nouns exactly as in instruction.
- Inference for `potential_obj`: Limited to 5 inferred objects to ensure relevance.
- Language Consistency: Use singular/plural as in instruction for mentioned objects; inferred objects use singular unless context suggests plural.

Examples

Example 1

Input:

```
{"instruction": "Go to the spa with one bed, brown tiles on the walls, a visible white radiator, and clean out the sink and bed"}
```

Output:

```
{"instruction": "Go to the spa with one bed, brown tiles on the walls, a visible white radiator, and clean out the sink and bed",  
"direct_obj": ["sink", "bed", "tiles", "radiator"],  
"potential_obj": ["towel", "tub"]}
```

Task

- Process the JSON input provided by me and return a complete JSON output adhering to the above requirements.
- Ensure the output is correctly formatted, readable, and both `direct_obj` and `potential_obj` are sorted by specified criteria.
- Wait for the my JSON input to process. Do not process sample inputs unless explicitly provided.

Figure 9: Prompt designed for object list extraction in spatial inference experiments, applied to non-fine-tuned LLMs (GPT-4o, Grok3, Gemini-2.5-Flash, Qwen3-4B). This structured prompt directs the LLM to accurately identify and enumerate task-relevant objects from navigation instructions. The same prompt is used for GPT-4o in REVERIE dataset experiments.

You are tasked with processing a JSON input containing navigation instructions and generating a new JSON output. The input JSON has the following structure:

```
{  
  "path": [string, ...],  
  "objId": number,  
  "heading": number,  
  "scan": string,  
  "path_id": string,  
  "instr_id": string,  
  "instruction": string  
}
```

Your goal is to create a valid JSON output that meets these requirements:

1. Retained Fields:

- Copy path, heading, scan, path_id, instr_id, and instruction from the input, unchanged.
- Exclude objId.

2. Final Destination Spatial Relations:

- Include exactly two strings:
 - First: Starts with "The destination is ..." and describes the final location based on the instruction (e.g., "the laundry room on the first level"). If the destination is unclear, use a generic description (e.g., "the specified location").
 - Second: Starts with "The spatial layout of the destination is ..." and infers a simple, typical layout for the destination type (e.g., for a laundry room, a shelf above a washing machine). Base inferences on common knowledge, avoiding overly specific assumptions.

3. Output Constraints:

- Include only the specified fields (path, heading, scan, path_id, instr_id, instruction, final_destination_spatial_relations).
- Ensure the output is a valid JSON object.
- Assume the input JSON is valid.

Example Input:

```
{  
  "path": [  
    "faa7088781e647d09df1d5b470609aa3",  
    "7d708a5b80ee45979870bae83b2bdd44",  
    "c29e99f090194613b5b11af906c47dab",  
    "aa4cf0126dd4c6a9c533ca9cb4a033d",  
    "5bc41a6e3b7748149e0e8592c5b4d142",  
    "3f432ddd169d4433979e004d1237d029",  
    "3e51eeaac8404b31ad8a950bb2bb953d"  
  ],  
  "objId": 156,  
  "heading": 0.32,  
  "scan": "cV4RVeZvu5T",  
  "path_id": "7172_156",  
  "instr_id": "7172_156_0",  
  "instruction": "Go to the laundry room on the first level and remove the leopard trinket from the shelf"  
}
```

Example Output:

```
{  
  "path": [  
    "faa7088781e647d09df1d5b470609aa3",  
    "7d708a5b80ee45979870bae83b2bdd44",  
    "c29e99f090194613b5b11af906c47dab",  
    "aa4cf0126dd4c6a9c533ca9cb4a033d",  
    "5bc41a6e3b7748149e0e8592c5b4d142",  
    "3f432ddd169d4433979e004d1237d029",  
    "3e51eeaac8404b31ad8a950bb2bb953d"  
  ],  
  "heading": 0.32,  
  "scan": "cV4RVeZvu5T",  
  "path_id": "7172_156",  
  "instr_id": "7172_156_0",  
  "instruction": "Go to the laundry room on the first level and remove the leopard trinket from the shelf",  
  "final_destination_spatial_relations": [  
    "The destination is the laundry room on the first level.",  
    "The spatial layout of the destination is a shelf above a washing machine with the leopard trinket on it."  
  ]  
}
```

Task:

- Wait for the my JSON input to process.
- Generate a complete JSON output adhering to the requirements.
- Ensure the final_destination_spatial_relations field reflects the instruction's destination and a simple, typical layout

Figure 10: Prompt employed for destination spatial layout inference using GPT-4o in REVERIE experiments. This prompt directs the LLM to generate accurate spatial arrangements of objects at the target location.

Instruction: Walk down the stairs all the way and past the Christmas tree. Make a right turn and walk past the blue chair into the room with the white sink.

History: step 0: go down to Place 3 which is corresponding to Image 3 (Omitted for brevity)

Trajectory: Place 0 3 4 5 6 8 9 10 12 18 20 22 18 19 28

Map:

Place 0 is connected with Places 1, 2, 3, 4
 Place 3 is connected with Places 5, 4, 0, 2
 Place 4 is connected with Places 6, 5, 0, 3
Place 5 is connected with Places 6, 3, 4
 Place 6 is connected with Places 7, 8, 5, 4
 Place 8 is connected with Places 9, 10, 6, 7
 (Omitted for brevity)

Supplementary Info: (Omitted for brevity)

Previous Planning: (Omitted for brevity)

Possible Destination Info (For reference only, may not be completely accurate)

The destination is the bathroom, positioned in front of the sink. The spatial layout of the destination includes a sink directly in front, a toilet positioned to the left, and a shelf located to the right and above.

Action Options (step 14): ['A. stop', ...'D. go up to Place 6 which is corresponding to Image 6', ...]

Thought: ...Based on the map, I need to explore connected places to find the room with the white sink. **The possible destination info suggests a bathroom layout...**

New Planning: 1. Turn left to Place 28. 2. Explore connected places to find the room with the white sink.

Action: "D"

Pruning Scores Detail (Step 15, Current VP: 77ab37bf2249afa1a9d30d736a00b (Place 19))

Node be3d7ae0352d481191e4c9e351e71b08 (Place 0):
 Raw: age=15, deg=4, unexpl_neigh=2, dist=N/A
 Contrib: time=5.00 (eff_age=5), deg=8.00, front=-10.00, dist=0.00
 Total Score: -13.00

Node be7a60657d6483996aa2f0d03b9d691 (Place 3):
 Raw: age=14, deg=4, unexpl_neigh=1, dist=N/A
 Contrib: time=4.00 (eff_age=4), deg=8.00, front=-5.00, dist=0.00
 Total Score: -9.00

Node f17bd928d5c84ebbb4d2d8806682f4af (Place 4):
 Raw: age=13, deg=4, unexpl_neigh=0, dist=N/A
 Contrib: time=3.00 (eff_age=3), deg=8.00, front=0.00, dist=0.00
 Total Score: -5.00

Node 80befc44c6d14348a3f9bda8ba719d70 (Place 5):
 Raw: age=12, deg=3, unexpl_neigh=0, dist=N/A
 Contrib: time=2.00 (eff_age=2), deg=6.00, front=0.00, dist=0.00
 Total Score: -4.00

Node 024edcc6db70425aaa54f5596b0ebda8 (Place 6):
 Raw: age=11, deg=4, unexpl_neigh=1, dist=N/A
 Contrib: time=1.00 (eff_age=1), deg=8.00, front=-5.00, dist=0.00
 Total Score: -12.00



Place 19 (current)



Place 0



Place 3



Place 5 for pruning



Place 4



Place 6

Figure 11: Step 15 in a Successful Case Study of MSNav. Spatial Module, based on the instructions, accurately and precisely describes information related to the final destination and the relationships of surrounding objects. By highlighting scene objects (e.g., pictures, lamps). The field 'Pruning Scores Detail' illustrates the complete calculation process and the resulting pruned nodes from Memory Module's dynamic pruning. As the current navigation point is already located in a downstairs room, MSNav removes the upstairs navigation point place 5.

Instruction: Walk down the stairs all the way and past the Christmas tree. Make a right turn and walk past the blue chair into the room with the white sink.

History: step 0: go down to Place 3 which is corresponding to Image 3 (Omitted for brevity)

Trajectory: Place 0 3 4 5 6 8 9 10 12 18 20 22 18 19 28

Map:

Place 0 is connected with Places 1, 2, 3, 4
 Place 3 is connected with Places 4, 0, 2
Place 4 is connected with Places 6, 0, 3
 Place 6 is connected with Places 7, 8, 4
 Place 8 is connected with Places 9, 10, 6, 7
 (Omitted for brevity)

Supplementary Info: (Omitted for brevity)

Previous Planning: (Omitted for brevity)

Possible Destination Info (For reference only, may not be completely accurate)

The destination is the bathroom, positioned in front of the sink. The spatial layout of the destination includes a sink directly in front, a toilet positioned to the left, and a shelf located to the right and above.

Action Options (step 15): ['A. stop', ...'D. turn right to Place 30 which is corresponding to Image 30', ...]

Thought: ...Based on the map, I should explore the connected places to find this room. **The possible destination info suggests a bathroom layout, which might be in one of the unexplored connected places. ...**

New Planning: 1. Turn right to Place 30. 2. Check for the room with the white sink.

Action: "D"

Pruning Scores Detail (Step 16, Current VP: ccfdfc7612ee4530887682d5e9c8e279 (Place 28))

Node be3d7ae0352d481191e4c9e351e71b08 (Place 0):
 Raw: age=16, deg=4, unexpl_neigh=2, dist=N/A
 Contrib: time=6.00 (eff_age=6), deg=8.00, front=-10.00, dist=0.00
 Total Score: -12.00

Node be7a60657d6483996aa2f0d03b9d691 (Place 3):
 Raw: age=15, deg=3, unexpl_neigh=1, dist=N/A
 Contrib: time=5.00 (eff_age=5), deg=6.00, front=-5.00, dist=0.00
 Total Score: -6.00

Node f17bd928d5c84ebbb4d2d8806682f4af (Place 4):
 Raw: age=14, deg=3, unexpl_neigh=0, dist=N/A
 Contrib: time=4.00 (eff_age=4), deg=6.00, front=0.00, dist=0.00
 Total Score: -2.00

Node 024edcc6db70425aaa54f5596b0ebda8 (Place 6):
 Raw: age=12, deg=3, unexpl_neigh=1, dist=N/A
 Contrib: time=2.00 (eff_age=2), deg=6.00, front=-5.00, dist=0.00
 Total Score: -9.00

Node 61aa577f8ebf40dd9bc04e27b1a4c80f (Place 8):
 Raw: age=11, deg=4, unexpl_neigh=1, dist=N/A
 Contrib: time=1.00 (eff_age=1), deg=8.00, front=-5.00, dist=0.00
 Total Score: -12.00



Place 28 (current)



Place 0



Place 3



Place 4 for pruning



Place 6



Place 8

Figure 12: Step 16 follows by Step 15 in this successful case study. The navigation point removed during the pruning in step 15 (Place 5) has already been removed from the set of active nodes considered in this step's memory/map. Memory Module now initiates a new round of dynamic pruning. From the five navigation points currently under consideration, Place 4 is identified and subsequently removed.

Instruction: Walk down the stairs all the way and past the Christmas tree. Make a right turn and walk past the blue chair into the room with the white sink.

History: step 0...step 22: turn left to Place 9 which is corresponding to Image 9

Trajectory: Place 0 3 4 5 6 8 9 10 12 18 20 22 20 18 19 28 30 29 32 33 31 19 11 9

Map:

Place 9 is connected with Places 11, 13, 14, 15, 7

Place 18 is connected with Places 20, 21, 19, 15

Place 20 is connected with Places 23, 24, 18, 25, 26
(Omitted for brevity)

Supplementary Info: (Omitted for brevity)

Previous Planning: (Omitted for brevity)

1. Turn left to Place 9. 2. Explore connected places to find the room with the white sink.

Possible Destination Info (For reference only, may not be completely accurate):

The destination is the bathroom, positioned in front of the sink. The spatial layout of the destination includes a sink directly in front, a toilet positioned to the left, and a shelf located to the right and above.

Action Options (step 23): ['A. stop', ... 'F. turn left to Place 14 which is corresponding to Image 14', ...]

Thought: I am currently at Place 9, and I need to find the room with the white sink. According to the map, Place 9 is connected to several places, including Place 11, 13, 14, 15, and 7. I have previously explored Place 11, which did not have the white sink. I should explore a new place connected to Place 9 to find the room with the white sink.

New Planning: 1. Turn left to Place 14. 2. Explore connected places to find the room with the white sink.

Action: "F"

Pruning Scores Detail (Step 24, Current VP: 7a489c31ceb14eca8783e4f1d8dc1c41 (Place 9))

Node 0acbbb92572f437faef8da9b991412f6 (Place 18):
Raw: age=11, deg=4, unexpl_neigh=2, dist=N/A
Contrib: time=1.00 (eff_age=1), deg=-8.00, front=-10.00, dist=0.00
Total Score: -17.00

Node 595344b8d6a7471691be526b8b9d685f (Place 20):
Raw: age=12, deg=5, unexpl_neigh=4, dist=N/A
Contrib: time=2.00 (eff_age=2), deg=-10.00, front=-20.00, dist=0.00
Total Score: -28.00




Figure 13: The final step in the successful case study of MSNav. Memory Module continued its dynamic pruning process after step 15 to the final step. Leveraging the precise destination information and object visual enhancements inferred by Spatial Module, MSNav successfully selected the crucial Action in this step: F. turn left to Place 14 which is corresponding to Image 14. Ultimately, the agent successfully reached the intended destination after a total of 25 steps.

Instruction: Turn right to exit the room. Turn right when you get to the end of the hallway. Walk toward the couches and stop there by the couches.

History: step 0: turn right to Place 3 which is corresponding to Image 3, step 1: go forward to Place 6 which is corresponding to Image 6

Trajectory: Place 0 3 6

Map:

Place 0 is connected with Places 1, 2, 3, 4

Place 3 is connected with Places 5, 6, 7, 4, 0

Place 6 is connected with Places 5, 8, 9, 10, 3

Supplementary Info:

Place 1, which is corresponding to Image 1

Place 2, which is corresponding to Image 2

Place 4, which is corresponding to Image 4

Place 7, which is corresponding to Image 7

Previous Planning:

1. Turn right to Place 3 to exit the room. 2. Turn right at the end of the hallway by going forward to Place 6. 3. Walk toward the couches and stop there.

Possible Destination Info (For reference only, may not be completely accurate):

The destination is the living room, located near the couches. The spatial layout of the destination includes couches, primarily located on the left side, adorned with numerous pillows, a table situated nearby, and a vase also being present.

Action Options (step 2): ['A. turn left to Place 5 which is corresponding to Image 5', 'B. turn left to Place 8 which is corresponding to Image 8', 'C. turn left to Place 9 which is corresponding to Image 9', 'D. turn right to Place 10 which is corresponding to Image 10', 'E. turn around to Place 3 which is corresponding to Image 3']

Thought: I have turned right to exit the room and then turned right at the end of the hallway. Now, I need to walk toward the couches and stop there. The Possible Destination Info suggests that the destination includes couches with pillows and a nearby table. From the current options, Place 8, corresponding to Image 8, shows a sofa chair and side table, which aligns with the description of the destination.

New Planning: 1. Turn left to Place 8 to approach the couches. 2. Stop near the couches as it matches the destination description.

Action: "B"



Figure 14: The key step 2 of a failure case for MSNav. Following the instruction to navigate to the room with couches, after executing the initial steps, MSNav, at step 2, selected the action to proceed to Place 8 based on the possible destination information (describing the living room and couches). However, this choice did not successfully guide the agent to ultimately reach the specific couch destination specified in the instruction.

Instruction: Turn right to exit the room. Turn right when you get to the end of the hallway. Walk toward the couches and stop there by the couches.
History: step 0: turn right to Place 3 which is corresponding to Image 3, step 1: go forward to Place 6 which is corresponding to Image 6, step 2: turn left to Place 8 which is corresponding to Image 8

Trajectory: Place 0 3 6 8

Map:

Place 0 is connected with Places 1, 2, 3, 4
 Place 3 is connected with Places 5, 6, 7, 4, 0
 Place 6 is connected with Places 5, 8, 9, 10, 3
 Place 8 is connected with Places 11, 12, 13, 6, 5

Supplementary Info:

Place 1, which is corresponding to Image 1
 Place 2, which is corresponding to Image 2
 Place 4, which is corresponding to Image 4
 Place 7, which is corresponding to Image 7
 Place 9, which is corresponding to Image 9
 Place 10, which is corresponding to Image 10

Previous Planning:

1. Turn left to Place 8 to approach the couches. 2. Stop near the couches as it matches the destination description.

Possible Destination Info (For reference only, may not be completely accurate):

The destination is the living room, located near the couches. The spatial layout of the destination includes couches, primarily located on the left side, adorned with numerous pillows, a table situated nearby, and a vase also being present.

Action Options (step 3): ['A. stop', 'B. turn left to Place 11 which is corresponding to Image 11', 'C. go forward to Place 12 which is corresponding to Image 12', 'D. turn right to Place 13 which is corresponding to Image 13', 'E. turn around to Place 6 which is corresponding to Image 6', 'F. turn around to Place 5 which is corresponding to Image 5']

Thought: I have reached Place 8, which matches the description of the destination with couches and a side table. The instruction was to stop by the couches, and the previous planning also indicated that Place 8 is the destination. Therefore, I should stop here.

New Planning: Stop at Place 8 as it matches the destination description with couches and a side table.

Action: "A"



Intended Destination



Actual Destination (Place 8)

Figure 15: The final step of the failure case for MSNav. Following the instruction to navigate to the room with couches, after executing the first two steps to reach Place 8, MSNav, at step 3, mistakenly determined that the current location (Place 8) was the final destination based on its internal planning and possible destination information, and chose to stop. As the agent failed to reach the actual couch destination specified in the instruction, this navigation attempt ultimately failed.